Proposal for an experiment at GSI

Two-proton decay of ^{19}Mg

(the experiment S271 accepted on 13/12/2001)

T. Aumann,[1], L. Batist[2], J. Döring[1], H. Geissel[1], V. Z. Goldberg[3], L. Grigorenko[1,4], Z. Janas[5], O. Kisselev,[1,2], H. Kumagai[6], C. Mazzocchi[1], I. Mukha[1,4], A. Ozawa[6], M. Pfützner[5], E. Roeckl[1], G. Schrieder[7], K. Sümmerer[1], O. Tarasov[8], H. Weick[1]

10 November, 2002

[1] GSI, Planckstr. 1, D-64291 Darmstadt
[2] St. Petersburg Nuclear Physics Institute, RU-188350 Gatchina, Russia
[3] University of Notre Dame, Notre Dame, USA
[4] Kurchatov Institute, RU-123182 Moscow, Russia
[5] Institute of Experimental Physics, Warsaw University, PL-00681 Warsaw, Poland
[6] RIKEN, Hirosawa 2-1, Wako, Saitama 351-0198, Japan
[7] Istitut für Kernphysik , TUD, D-64289 Darmstadt
[8] NSCL, Michigan State University, MI48824-1321, USA

Abstract

We propose a search for the two-proton decay of the ground state of ^{19}Mg by using a ^{20}Mg beam produced at the Projectile Mass Separator (FRS). The ^{19}Mg decay will be measured in-flight by detecting the triple ^{17}Ne+p+p coincidence. The ^{19}Mg ground-state is a prospective candidate for observation of "direct" two-proton radioactivity. Extensive studies made in the framework of a realistic three-body model predict its half-life to be 0.5–700 ps which overlaps reasonably with the decay-time range measurable at FRS. We intend to observe the direct proton emission and to measure the half-life of ^{19}Mg, its decay energy as well as proton-proton correlations. The half-life value will be derived from the distribution of the ^{19}Mg decay vertices. The vertices will be extrapolated from measured (by means of silicon micro-strip detectors) trajectories of all fragments. In addition, exploratory studies of the possible two-proton emitters ^{30}Ar and ^{34}Ca can be performed simultaneously with the ^{19}Mg decay measurements. The beam time request is 29 shifts divided in two runs. For the first run, we need 16 shifts of 350 MeV/u ^{24}Mg primary beam from SIS with an intensity of 10^{10} ions per spill. For the second run, we request 13 shifts of 650 MeV/u of ^{40}Ca beam with an intensity 10^{10} ions per spill.

Spokesperson: I. Mukha
GSI contact persons: K. Sümmerer

1 Experimental method

Direct (Coulomb-delayed) two-proton radioactivity of long-lived states, or a spontaneous break-up of elements with emission of two protons (2p), remains rather unexplored issue though it

had been predicted to exist near the proton drip-line long time ago [1]. The experiments, aimed to find such an exotic nuclear decay, generally use the ion-implantation or the in-flight decay method. In the former case, a radioactive nucleus is first stopped and its activity is measured subsequently. Recently, the first evidence for radioactivity of ^{45}Fe ground state was obtained at GSI [2] and GANIL [3] using this method.[1] The conventional in-flight decay method aims at detecting all fragments of a 2p-precursor in missing-mass or invariant-mass measurements. We propose another type of in-flight decay experiment in which all fragments are *tracked* and the decay vertices are recovered from the measured trajectories. Such a tracking technique has proven to be a precise and effective tool in measurements of Coulomb fragmentation of ^{8}B with the KaoS setup at GSI [4].

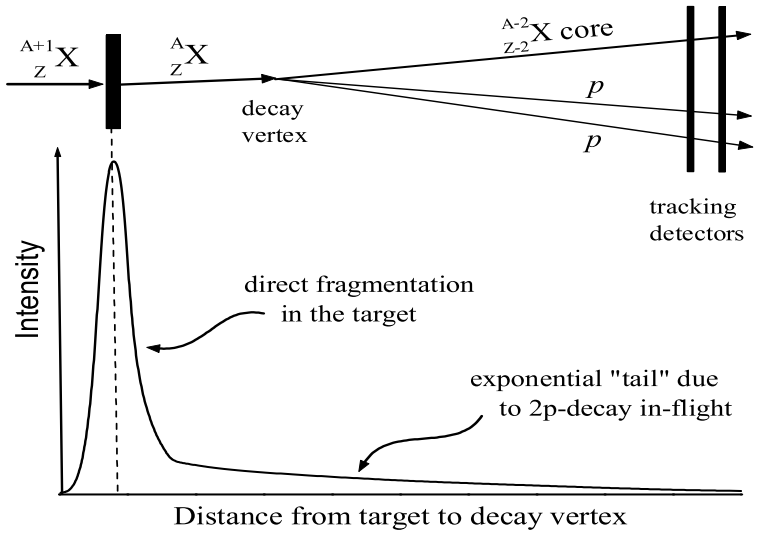

Figure 1: Measurements of a two-proton decay in-flight. Upper panel: schematic layout of detectors. Lower panel: distribution of decay vertices reconstructed from data of the tracking detectors.

The idea of in-flight decay experiment is discussed in [5] and sketched in Fig. 1. The 2p-precursor may be produced in a nuclear reaction, e.g. one-neutron knock-out, and the resulting state decays into the two protons and a heavy fragment after leaving the target area. If the directions of the decay products are measured by a pair of tracking detectors, the coordinates of each decay can be defined as a vertex of three fragment momenta. Thus the half-life of the initial nucleus can be derived by fitting the measured vertex distribution by an exponent function.[2] Positive features of this kind of experiment are a straightforward derivation of the lifetime and the simultaneous measurement of all correlations among the fragments.

The general problem in the search for two-proton radioactivity is the insufficient knowledge of atomic masses close to the proton drip-line. Uncertainties of 100–300 keV for 2p-decay energies result in variations of the expected half-lives by factor of 100–1000. The implantation experiments are feasible for half-life intervals from 10^{-6} s to 10^{-2} s (upper limit is estimated because of competition between 2p and β decays). The missing-mass or invariant-mass measurements work for half-lives less than 10^{-19} s, the respective widths being more than 10 keV. There is a gap of 13 orders of magnitude between the half-life intervals measurable by these two methods. The suggested technique, decay-in-flight experiments, allows to partly bridge this gap.

This situation is illustrated in Fig. 8, where the energy dependence of the half-life of several 2p-decay candidates is shown. The rectangles indicate the ranges of predicted decay energies and

[1] Though decay protons were not identified in the experiments, only a mechanism of 2p emission can explain the data.

[2] The measured vertex distribution should also contain a component from direct fragmentation of projectile nuclei in target which is centered at the target position. However, this component can be eliminated by a measurement of the nuclear charge of the reaction products straight after target.

respective half-life values. Details of the calculations are given in Section 1.2. For ^{45}Fe, the decay energy is taken from systematics [19], the experimental results [2, 3] are shown by the black box and circle, respectively. As can be seen from Fig. 8, ^{45}Fe can be studied with the implantation method only, whereas the relatively light nucleus ^{19}Mg is likely to decay within the time interval from 10^{-13} s to 10^{-6} s, which is well suited for the in-flight method.[3] We concentrate on this nucleus and discuss its properties in Section 1.2 in details.

1.1 Experimental data available

In the missing mass or the invariant-mass experiment, the excitation energy of the initial nucleus is recovered to assure that the registered events have the same decay energy. Several successful experiments have been performed to study two-proton (or other three-particle) decays in the light nuclei. These includes decays of ground states of ^{6}Be (α+2p) [11], ^{12}O (^{10}C+2p) [13], ^{16}Ne (^{14}O+2p) [14], and excited states of ^{9}Be*($5/2^{-}$ into n+2α) [12], ^{12}C*(1^{+} into 3α) [15]. Unfortunately, due to experimental problems and theoretical complexity most of these experiments do not allow a unique interpretation.

A recent example of the implantation method is the GSI experiment on decay of ^{45}Fe which is bound with respect to single-proton decay but unbound to 2p-decay. The ^{45}Fe atoms were produced by fragmentation reactions of a 650 MeV/u ^{58}Ni beam at FRS [2], and were implanted into a stack of silicon detectors, in which a subsequent radioactivity was measured. New digital front-end electronics was applied for measurements in the microsecond range in addition to the conventional millisecond range. Four events with an energy of about 1 MeV were observed within 10 ms after the time of ion implantation, with no γ or β emission in coincidence. This decay pattern is expected if the ^{45}Fe ground state decays by the emission of two protons to the ground state of ^{43}Cr. The respective half-life of $3.4^{+2.6}_{-1.1}$ ms and the 2p-decay energy of 1.1(1) MeV are derived. Similar results obtained at GANIL independently [3] are in quantitative agreement with the discussed data. Though protons were not identified in both experiments, the common conclusion is that only a mechanism of 2p-emission can explain the observed decay patterns. Fig. 8 includes also a comparison between the experimental data and the three-body model prediction (described in the next Section), indicating a quantitative agreement.

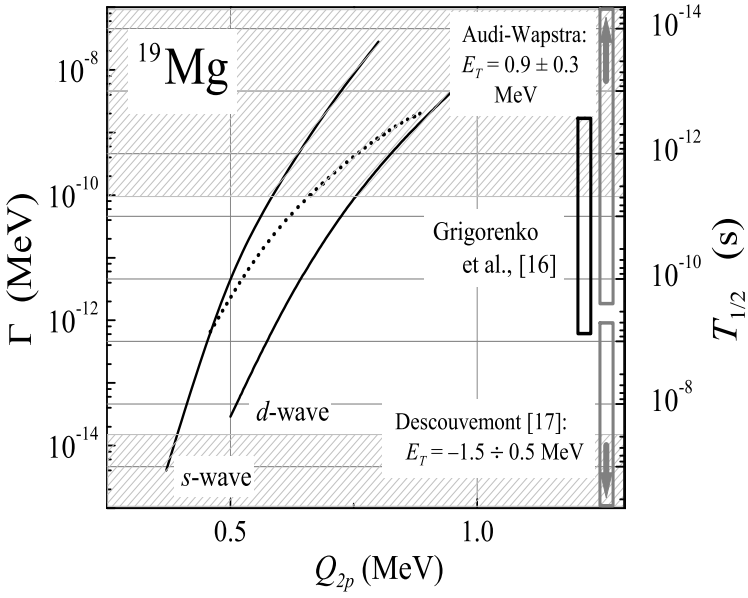

Figure 2: Width and half-life (right ordinate) versus the 2p-decay energy of ^{19}Mg. The solid curves are the three-body model predictions assuming different l^2 components dominating in the nucleus. Dotted curve takes into account the correct Coulomb displacement energy for a structure with mixed components. The upper hatched area corresponds to the half-lives which are too short for the decay-in-flight experiment (e. g. $T_{1/2}$ less than ∼5 ps), the lower hatched area corresponds to the long half-lives suited for an implantation.

[3]The similar predictions for the ^{30}Ar and ^{34}Ca nuclei shown in Fig. 8 are discussed in Appendix.

1.2 Mechanism of 2p decay and three-body model predictions for ^{19}Mg

In general case the two-proton decay can be described by three possible mechanisms: (i) sequential emission of protons via an intermediate state, (ii) simultaneous emission of protons, and (iii) "diproton emission", i.e. emission of a ^{2}He cluster, the latter disintegration mode being related to very strong *pp* correlations. The binding energy systematics [19] indicates that sequential emission of protons is likely to be energy forbidden ($S_{2p} < 0$, $S_p > 0$) in ^{19}Mg, and this nucleus belongs to the class of "true two-proton emitters" [1]. The phenomenon of the true two-proton emission is analogous in the sense of separation energy conditions to the "borromean" property of bound halo nuclei (e.g. ^{6}He, ^{11}Li [9], or ^{17}Ne [10]). It was discussed in [1], that the true two-proton emitters should generally have lifetimes much longer than sequential-proton emitters, and specific correlations between emitted protons were predicted with proton energies to be almost equal.

From theoretical point of view, a true two-proton emission is an extremely complicated process which has been treated by means of the simple quasi-classical "diproton" model for many years (see, for example, [8, 17]). Recently, the three-body quantum mechanical model [6] has been developed which incorporates both the (ii) and (iii) decay mechanisms in a natural way. The model has carefully been tested on the known three-particle decays of light nuclei [29]. It provides lifetimes as well as momentum correlations among the decay fragments.

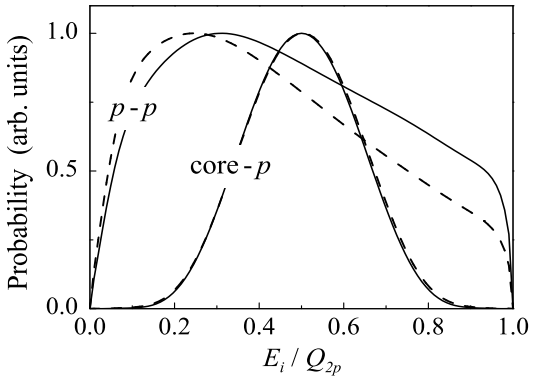

Figure 3: Relative energy distributions for ^{19}Mg decay products. E_i is the relative energy between p-p and ^{17}Ne-p, Q_{2p} is the ^{19}Mg decay energy. Solid-line and dashed-line curves were calculated assuming *s*-wave or *d*-wave component dominated in the ^{19}Mg ground state.

In paper [7], the method of [6] was applied to the prospective two-proton decay candidate ^{19}Mg. Calculated half-life of ^{19}Mg is shown in Fig. 2 versus decay energy. It has a significant uncertainty shown by two solid curves which is connected with a poor knowledge of the ^{19}Mg structure. Accurate estimates of the Coulomb displacement energy are also made, which reduce the half-life uncertainty predictions down to the range from 0.5 ps to 700 ps (see the dotted curve in Fig. 2). This range overlaps reasonably with the range accessible by suggested in-flight decay experiment.

An important information about decay mechanism is provided by energy correlations of decay fragments. The energy correlations between fragments, calculated for ^{19}Mg decay [7], are shown in Fig. 3. The p-p distribution is rather broad, though its maximum is at ∼200 keV. This enhancement is due to strong pairing interaction. The ^{17}Ne-p energy spectrum is peaked at about $0.5 \cdot E_T$ and does not depend on the initial structure. Thus energies of protons should be almost equal in agreement with the idea of Goldansky [1]. This allows to determine the total decay energy by using the maximum angle between proton and ^{17}Ne measured in fragmentation of ^{19}Mg.

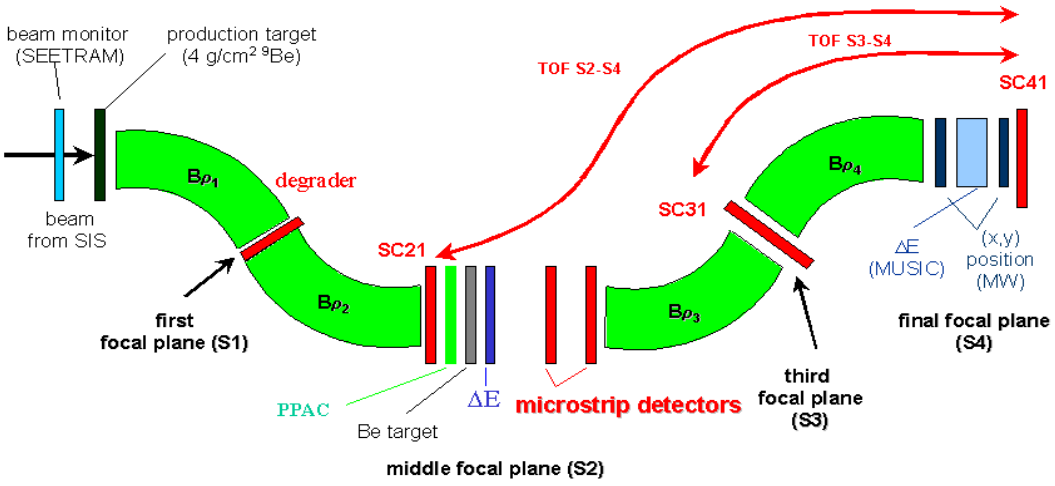

Figure 4: Sketch of set-up proposed to study the decays of ^{19}Mg, ^{30}Ar and ^{34}Ca in-flight. The secondary beams of ^{20}Mg, ^{31}Ar and ^{35}Ca are produced in a primary target and are selected by the first two magnet sections of the FRS. The 2p-precursors are populated in one-neutron knock-out reactions at the middle focal plane S2. Trajectories of all decay fragments are measured by micro-strip detectors at S2. In addition, the heavy fragments are detected and identified at the final focal plane S4.

2 The proposed experimental setup

The scheme of the proposed set-up is shown in Fig. 4. The radioactive ∼250 MeV/u ^{20}Mg beam will be produced at the Projectile Fragment Separator (FRS). The high beam energy is essential for the measurement of half-life down to the pico-second region. The FRS can provide both the large detection efficiency and high energy resolution required [22]. The first two stages of FRS will be set in achromatic mode needed for an optimal transmission of the ^{20}Mg ions, being stripped completely, and for focussing the ^{20}Mg beam on a secondary target. An achromatic degrader is planned be used in the first focal plane in order to reduce the rate of contaminant ions passing through the FRS. The ^{20}Mg charge will be identified by measuring energy losses in the scintillator detector SC21 in the central focal plane (S2) of FRS. The ^{20}Mg projectiles will be tracked by a stack of position-sensitive parallel-plane avalanche detectors, PPAC. The position information from PPACs, together with the magnetic field values from the FRS dipoles, will be used for a determination of the mass-to-charge ratio A/q for each ion thus allowing a selection of the mass-20 ions. The ^{19}Mg ground state will be populated in a secondary one-neutron knock-out reaction on a ^{9}Be target installed at S2. The ^{19}Mg decay products will be detected in triple coincidences ^{17}Ne+p+p. A precise determination of all fragment trajectories, needed to accurately reconstruct each decay vertex, will be achieved by means of two micro-strip detectors positioned just behind the target. The protons will be identified by their energy losses in micro-strip detectors. The last two stages of FRS will be set for an optimal transmission of heavy fragments ^{17}Ne. The ^{17}Ne ions will be identified at the final focal plane of FRS, S4, by means of the standard FRS detectors MUSIC (providing energy loss signals), multi-wire proportional chamber (X,Y position information), and scintillator detector SC41 providing a time-of-flight value when used in combination with SC21 or SC31. Trajectories and charges of all fragments will be measured at S2, and a vertex of each decay will be reconstructed allowing the determination of the ^{19}Mg half-life. A precise determination of all fragment trajectories will be achieved by means of two micro-strip detectors which were already used to study the Coulomb break-up of ^{8}B [4]. Each strip detector has a thickness of 300μm, an

active area of 56x56 mm^2, and a strip pitch of 100 μm.

The contribution of direct ^{20}Mg fragmentation in the target is expected to dominate in the registered triple coincidences ^{17}Ne+p+p. To suppress the detection of this component, a thin silicon detector ΔE will be positioned just after the target at S2. It provides the ion energy-loss information from which the nuclear charge can be determined. We intend to trigger only events when the ΔE signals are large sufficiently to yield unambiguous evidence that only magnesium (or at least no neon) isotopes exit the target. In combination with the triple coincidences registered by micro-strip detectors, this will prove that the registered decay events occur between the target and micro-strip detectors. Furthermore, an additional condition of registering heavy ions at the final focal plane S4 will dramatically reduce the data-acquisition trigger rate. For example, the total counting rate of the S2 detectors is estimated to be about 10^4 counts per spill with a 350 MeV/u primary beam of ^{24}Mg (see next Section), and the trigger rate should be 100 times less.

2.1 Monte Carlo simulations of experiment

We simulated the production of radioactive ions and their passage through the FRS by using the Monte Carlo programs MOCADI [23] and LISE^{++} [24].

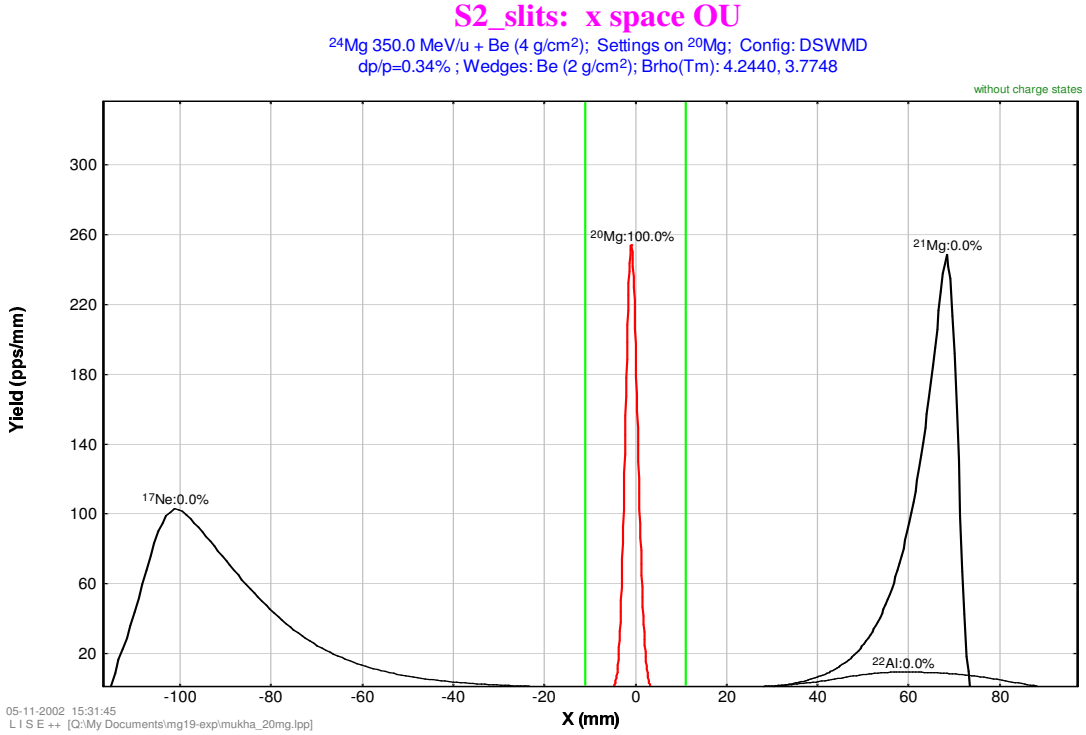

Figure 5: Monte Carlo simulation of radioactive ion distributions along the dispersion x-axis on the secondary target, at S2 (performed with the code LISE^{++} [24]).

For example, distributions of radioactive ions produced in fragmentation of ^{24}Mg are shown in Fig. 5 versus the dispersive axis X. One can see, that the ^{20}Mg beam can efficiently be selected before the secondary target using the FRS settings shown in figure.

The Monte Carlo program GEANT [25] was used to simulate nuclear decays and interactions of fragments with detectors and other materials of the suggested set-up. The main physics processes included in the simulations are, among others, energy loss due to ionization, multiple scattering, hadronic interaction and fluctuations of energy loss. The geometry (target thickness, ion energies, distances of silicon detectors from the secondary target *etc.*) was optimized in order to yield

the maximum accuracy in half-life determination combined with a high detection efficiency. For example, the simulated distribution of ^{19}Mg decay-vertices along the beam direction at S2 is shown in Fig. 6 by the dashed histogram. The assumed half-life value is $T_{1/2}$=20 ps.

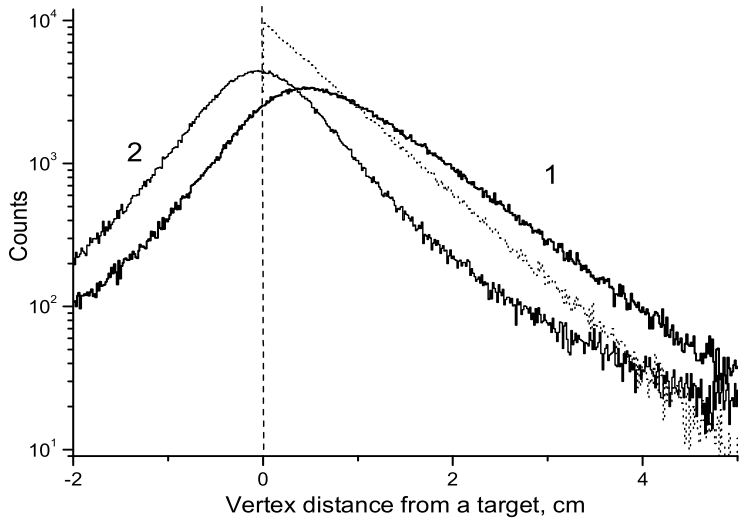

Figure 6: Monte Carlo simulation of the ^{19}Mg decay-vertex distributions with respect to the target. The dotted histogram shows the simulated ^{19}Mg decay coordinates with an assumed half-life of $T_{1/2}$=20 ps. The solid-line histogram 1 is the result of a reconstruction of the original distribution shown by the dotted histogram. The solid-line histogram 2 shows the result of reconstructed prompt decay of ^{19}Mg within the target.

In comparison with the experimental resolution achieved in the ^{8}B fragmentation experiment [4], the simulated spatial resolution is three times better (σ=0.4 cm). The angular straggling of fragments in the target was the main reason of the accuracy reported in [4]. In our case, the ^{20}Mg$\rightarrow^{19}$Mg fragmentation occurs in-flight out of the target, which is the main reason of the resolution improvement. Moreover, in our case there are three possible pairs of trajectories to be used in the vertex reconstruction, which allows a resolution improvement and can thus dramatically reduce a possible background. The simulated total efficiency of the detector setup registering the triple coincidences is on average 20% for $T_{1/2}$=20 ps.

2.2 Accuracy accessible in the life-time measurements

We have fitted the reconstructed vertex distributions, such as the one depicted in histogram 1 in Fig. 6, by an exponential function folded with the spatial resolution derived from the histogram 2 displayed in Fig. 6. The derived half-life values are shown in Fig. 7 for various assumed half-lives. Stars, squares and circles correspond to the different positions of the multi-strip detectors at distances of 4/14 cm, 14/31 cm, 45/60 cm after the target, respectively. As can be seen from the figure, the shortest half-life accessible with the suggested setup is of order of few pico-seconds. The best half-life accuracy can be achieved by an optimal choice of the positions of the multi-strip tracking detectors.

2.3 Advantages of the suggested experiment

1. In the preparations to this proposal, the dedicated theoretical studies have been performed to obtain the most reliable prediction of the ^{19}Mg half-life [7]. These studies are based on the new theoretical model proven to be accurate for all known nuclear three-particle decays [29]. The additional confirmation of reliability of the model is provided by the recent observation of the 2p-decay of ^{45}Fe [2].

2. In comparison with the implantation method where heavier nuclei such as ^{45}Fe are produced with intensities of few events per day, we propose to use the $\sim$1000 times more intensive

beam ^{19}Mg. The suggested method is exclusive because of the direct registration of protons and their correlations.

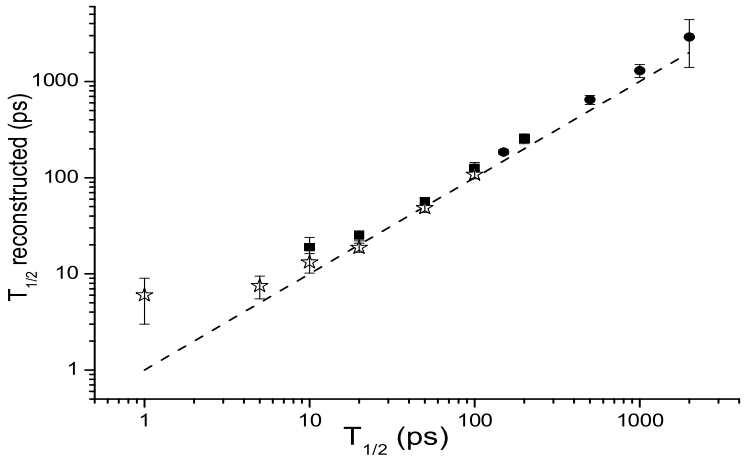

Figure 7: The ^{19}Mg half-life values derived from the reconstructed decay-vertex distributions like those shown in Fig. 2.1. For each half-live value $T_{1/2}$, 5000 decays of ^{19}Mg were simulated by GEANT. Stars, squares and circles correspond to the set-up layouts with the pair of multi-strip detectors positioned at 4/14 cm, 14/31 cm, 45/60 cm after the target, respectively.

3. The suggested method allows using much thicker secondary target in comparison with the missing mass, invariant mass methods (projectile straggling in a target does not affect a half-life determination). By performing the measurement at S2, severe losses of beam intensity are avoided, such as those occurring during beam transport to a remote cave. Contrary to the missing-mass and invariant-mass methods, the proposed method allows to measure the half-life of 2p-emitters. The range of accessible half-life overlaps reasonably well with the theoretical predictions.

4. The high energies of beams from FRS allow us to use a larger thickness of the secondary target than that possible at other facilities. For example, we expect to to use a 40-80 times thicker secondary target than the recent experiment at GANIL [20]. As the simulated efficiency of the detector setup is by factor 5 times higher than that used in the GANIL experiment, the suggested experiment promises to be about 200-400 times more sensitive.

3 Production of ^{19}Mg at the FRS and beam-time estimates

The ^{19}Mg nuclei will be produced in one-neutron stripping reaction of a ^{20}Mg beam which will be obtained by fragmentation of a ^{24}Mg or ^{40}Ca primary beam on a ^{9}Be target. The respective estimates are shown in the Table 3. The last column lists the estimated decay rates of interest.

We expect to register about 40 2p-decays of ^{19}Mg per hour in case of fragmentation of ^{20}Mg assuming the respective cross-section to be 0.3 mb. This is a conservative estimate, as the EPAX calculations [27] predict a sum cross-section of 45 mb for the reactions ^{12}C(^{20}Mg, Ne) while the experimental value is 123(9) mb at $\sim$ 1 GeV/u [26] and 350(80) mb at 43 MeV/u [20].

Thus we expect to measure the ^{19}Mg decay by accumulating of $\sim$4000 events in 13 shifts during the first experiment with a ^{24}Mg primary beam. Calibration measurements, tuning of the FRS *etc.* require 3 shifts.

In the second experiment we propose to use a ^{40}Ca primary beam of higher energy, i. e. 650 MeV/u. In this case we expect a higher counting rate of ^{19}Mg, and smaller values of its half-life are accessible (though measurements will be more difficult because of smaller energy losses of protons in the micro-strip detectors). In addition, a simultaneous detection of possible 2p-decays of the ^{34}Ca and ^{30}Ar nuclei will be feasible in this case (see Appendix).

Table 1: Estimate of production rates of ^{19}Mg by using [27]. The ^{24}Mg or ^{40}Ca beam intensity is 10^{10} ions per spill, and the thickness of primary ^{9}Be target is 4 g/cm^2 or 6 g/cm^2, respectively. Production rates of the ^{30}Ar and ^{34}Ca nuclei which can be measured simultaneously with ^{19}Mg are given as well.

Energy MeV/u	Primary reaction	σ_1, μb	Intensity at S2, ions/spill	Secondary reaction	Target ^{9}Be, g/cm^2	σ_2, μb	Production rate, per 100 spills
350	^{9}Be(^{24}Mg,^{20}Mg)4n	5.7	1000	^{9}Be(^{20}Mg,^{19}Mg)n	1.8	0.3	11
650	^{9}Be(^{40}Ca,^{20}Mg)4n	1.6	3400	^{9}Be(^{20}Mg,^{19}Mg)n	3.6	0.3	18
650	^{9}Be(^{40}Ca,^{35}Ca)5n	0.05	70	^{9}Be(^{35}Ca,^{34}Ca)n	3.6	0.2	0.3
650	^{9}Be(^{40}Ca,^{31}Ar)α5n	0.03	40	^{9}Be(^{31}Ar,^{30}Ar)n	3.6	0.2	0.13

In summary, we request 29 shifts in two runs. In the first run, we need 16 shifts of 350 MeV/u primary beam of ^{24}Mg from SIS with an intensity of 10^{10} ions per spill. In the second run, we request 13 shifts of 650 MeV/u primary beam ^{40}Ca from SIS with intensity of 10^{10} ions per spill.

4 Appendix. Exploratory study of ^{30}Ar and ^{34}Ca 2p-decays

In Fig. 8, the half-lives of ^{30}Ar and ^{34}Ca calculated by the three-body model [7] are shown in comparison with those of ^{19}Mg and ^{45}Fe. The decay energy around 1.2 MeV predicted for ^{30}Ar by [19] fits well to in-flight decay experiment. However, the energy 1.8 MeV given by [30] should cause a very short half-life of 10^{-15} s. For ^{34}Ca, the 2p-decay energy 2.2 MeV estimated in [30] is close to the limit of in-flight experiment. However, the respective prediction from systematics [19], 1.4 MeV, results in the very long half-life. The latter is apparently incorrect as the ^{34}Ca half-life is known to be shorter then 35 ps [31]. Thus the ^{34}Ca decay can most probably not be measured by the implantation method, however there is a chance to study it in an in-flight experiment.

With a 650 MeV/u primary beam of ^{40}Ca, the FRS settings should be practically the same for ^{19}Mg, ^{34}Ca and ^{30}Ar measurements. The corresponding intensity estimates of ^{34}Ca and ^{30}Ar are given in Table 3. Though only a few decay events are expected to be registered, a valuable information about the ^{34}Ca and ^{30}Ar properties may still be obtained.

References

[1] V.I. Goldansky, Nucl. Phys. **19**, 482 (1960).
[2] M. Pfützner et al., Eur. Phys. J., **A14**, 279 (2002).
[3] J. Giovinazzo et al., Phys. Rev. Lett., **89**, 102501 (2002).
[4] N.Iwasa et al., Phys. Rev. Lett. **83**, 2910 (1999).
[5] I.G. Mukha and G. Schrieder, Nucl. Phys. **A690** 280c (2001).
[6] L.V. Grigorenko, R.C. Johnson, I.G. Mukha, I.J. Thompson, and M.V. Zhukov, Phys. Rev. Lett. **85**, (2000) 22; Phys. Rev. **C64** (2001) 054002.
[7] L. Grigorenko, I. Mukha and M. Zhukov, "Prospective candidates for the two-proton decay studies: (I) Structure and Coulomb energies of ^{17}Ne and ^{19}Mg", Nucl. Phys. A, in print; "Prospective candidates for the two-proton decay studies: (II) Exploratory studies of ^{30}Ar, ^{34}Ca and ^{45}Fe", submitted to Nucl. Phys. A.
[8] B.A. Brown, Phys. Rev. **C43**, R1513 (1991).
[9] M.V. Zhukov *et al.*, Phys. Rep. **231**, 153 (1993).

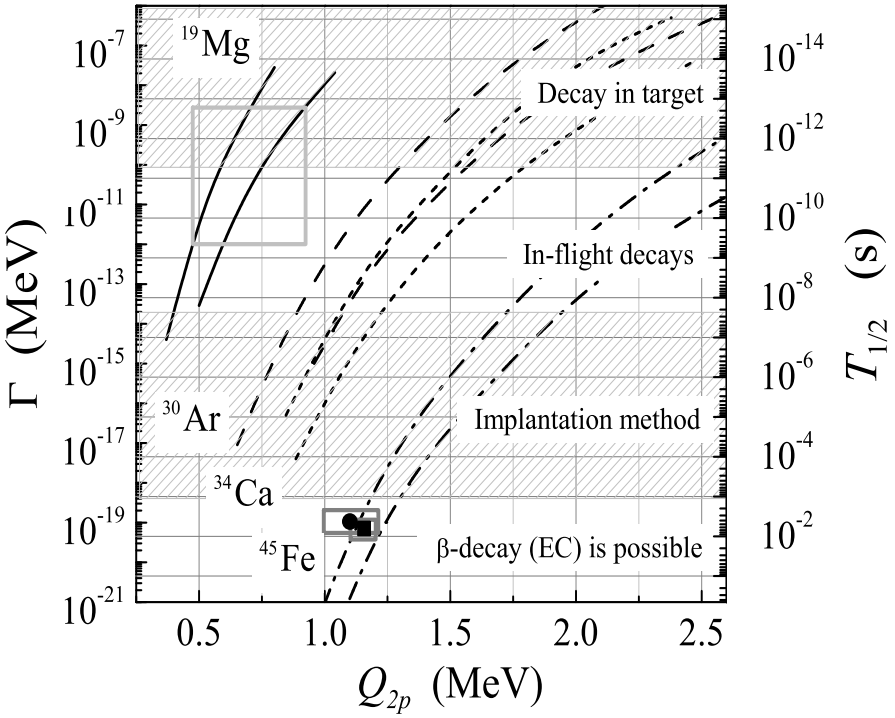

Figure 8: Width or half-life versus the decay energy. Solid, dashed, dotted and dash-dotted curves form "corridors" of possible half-life values for ^{19}Mg, ^{30}Ar, ^{34}Ca, and ^{45}Fe, respectively.

[10] M.V. Zhukov and I.J. Thompson, Phys. Rev. **C52**, 3505 (1995).
[11] O.V. Bochkarev *et al.*, Nucl. Phys. **A505**, 215 (1989).
[12] O.V. Bochkarev *et al.*, Sov. J. Nucl. Phys. **52**, 1525 (1990);
G. Nyman *et al.* , Nucl. Phys. **A510**, 189 (1990).
[13] R. A. Kryger *et al.*, Phys. Rev. Lett. **74**, 860 (1995).
[14] G. J. KeKelis *et al.*, Phys. Rev. C **17**, 1929 (1978).
[15] D.P. Balamuth, R.W. Zurmühle, and S.L. Tabor, Phys. Rev. C **10**, 975 (1974).
[16] A.A. Korsheninnikov, Sov. J. Nucl. Phys. **52**, 827 (1990).
[17] W. Nazarewicz *et al.*, Phys. Rev. **C53**, 740 (1996).
[18] B. Blank *et al.*, Phys. Rev. Lett. **84**, 1116 (2000).
[19] G. Audi and A.H. Wapstra, Nucl. Phys. **A565** (1993) 1; **A595** 409 (1995).
[20] T. Zerguerras, Ph.D. thesis, IPN Orsay (2001), unpublished.
[21] L. Grigorenko, I. Mukha, I. Thompson and, M. Zhukov
Phys. Rev. Lett. **88**, 042502 (2002).
[22] H. Geissel et al., Nucl. Instr. and Meth. **B70** 286 (1992).
[23] N. Iwasa et al., Nucl. Instr. Meth. **B126** 284 (1997).
[24] O.B. Tarasov, D. Bazin, M. Lewitowicz, O. Sorlin , Nucl. Phys. **A701** (2002) 661.
[25] "GEANT - detector description and simulation tool". CERN software library, http://wwwinfo.cern.ch/asd/geant.
[26] L.V. Chulkov et al., Nucl. Phys. **A603** 219 (1996).
[27] K. Sümmerer and B. Blank, Phys. Rev. **C61**, 034607 (2000).
[28] I. Mukha, AIP Proceedings **518**, 144 (2000).
[29] L.V. Grigorenko, I.G. Mukha, I.J. Thompson, M.V. Zhukov, Eur. J. Phys. A, in print.
[30] B.J. Cole, Phys. Rev. **C56** 1866 (1997).
[31] F. Pougheon, private communication, from NNDC, BNL, USA.